Available online at www.sciencedirect.com

ScienceDirect

Procedia CIRP 68 (2018) 499 – 504

www.elsevier.com/locate/procedia

19th CIRP Conference on Electro Physical and Chemical Machining, 23-27 April 2018, Bilbao, Spain

A Novel Modeling Approach for the Simulation of Precise Electrochemical Machining (PECM) with Pulsed Current and Oscillating Cathode

Fritz Klocke[a,b], Lukas Heidemanns[a,]*, Markus Zeis[b], Andreas Klink[a]

[a]*Laboratory for Machine Tools and Production Engineering (WZL) of RWTH Aachen University, Steinbachstr. 19, 52074 Aachen, Germany*
[b]*Fraunhofer-Institute for Production Technology IPT, Steinbachstr. 17, 52074 Aachen, Germany*

* Corresponding author. Tel.: +49-241-80-28007; fax: +49-241-80-22293. *E-mail address:* l.heidemanns@wzl.rwth-aachen.de

Abstract

Simulation in electrochemical machining (ECM) offers the capability to distinctly reduce time and costs of the design process and, thereby, increase the economic potential of the manufacturing technology. In recent years, different models for the simulation of ECM with direct current (DC-ECM) have been introduced and successfully applied to varying geometries. Furthermore, first approaches to model the effect of ECM with pulsed current have been presented. However, state of the art machine tools additionally apply an oscillation of the cathode to further improve surface quality and machining precision. To date there exists no validated model for this precise ECM (PECM) process.
Therefore, this paper outlines the challenges emerging from considering cathode oscillation in ECM simulation models. Based on an overview of existing models for ECM with pulsed current, conclusions are drawn which concepts can be adopted for the modeling of precise ECM and which phenomena require the introduction of new approaches. Lastly, a model for the simulation of precise ECM is presented. This model accounts for the flow field of the electrolyte, the evolution of temperature in the machining gap as well as the resulting electrical field and finally the material removal.

Peer-review under responsibility of the scientific committee of the 19th CIRP Conference on Electro Physical and Chemical Machining

Keywords: Type your keywords here, separated by semicolons ;

1. Introduction

ECM combines a high material removal rate with almost no tool wear and no thermally or mechanically damaged rim zone. These benefits are detracted by an intensive tool development process and high initial investment cost for machine tools. In recent years, the increased use of highly heat resisting materials in aircraft engines as well as rising demand for turbomachinery components has led to a revival of the ECM technology [1]. Besides the classic DC-ECM process two process variations have been developed. On the one hand, the pulsed ECM process applies a pulsed electrical source to allow a renewal of the electrolyte during pulse interval time. Thereby, a higher current density is realized which in turn leads to an increased accuracy and a decreased surface roughness. On the other hand, the PECM process amplifies these characteristics by adding an oscillating cathode movement. Electric pulses are only applied around the bottom dead center (BDC) of the oscillation while the larger working gap around the top dead center (TDC) allows an improved electrolyte flow. Both process variations result in a reduced material removal rate since the effective machining time is significantly reduced. Hence, they are primarily used as a finishing operation after roughing by DC-ECM or conventional technologies.

Simulation of the ECM process has been identified as a promising approach to reduce tool development costs and duration [2]. For the DC-ECM process comprehensive two-dimensional models have been developed, successfully validated and used for the cathode design of turbine blades [3]. However, the transfer to three dimensions is still hindered due to immense computational costs. In contrast, there does not yet exist a validated model for the PECM process. Due to the different time scales of the involved physical phenomena it is practically impossible to simply apply existing ECM models

Peer-review under responsibility of the scientific committee of the 19th CIRP Conference on Electro Physical and Chemical Machining
doi:10.1016/j.procir.2017.12.081

and simulate each individual current pulse of a typical PECM machining task [4]. Instead, short-cut methods have to be developed that enable a time efficient simulation. Therefore, this paper presents existing modeling approaches for the ECM and PECM process and assesses their advantages and shortcomings. Subsequently, a novel modeling approach is deducted and applied to a reference geometry. The last section evaluates the simulation results.

Abbreviations

BDC	bottom dead centre
BoP	begin of pulse packet
DC-ECM	ECM with direct current
ECM	electrochemical machining
EoP	end of pulse packet
PECM	precise electrochemical machining
TDC	top dead centre

2. Existing models of the ECM process

First models of the ECM process concentrated on the electrical field as the main physical phenomenon of the process. This let to the cos(φ)-method introduced by Tipton which relates the gap width to the angel of the cathode surface [5]. Later the influence of the temperature field and the gas evolution [6] as well as the velocity field [7] on the electric conductivity were included. While these models all described the equilibrium working gap the increased computational capacity enabled the transit simulation of the ECM progress at the beginning of this century [8]. By now, models for the cathode design for engine blades have been validated [3] even though they have not yet been implemented in industrial design processes. Other authors explicitly modelled the occurring chemical reactions as well as multi-ion transport [9]. However, these aspects have only been validated at a machining task in the range of micrometers and the necessity of these computationally costly models may be challenged due to the successful validation of the afore mentioned simpler models.

In general, the developed models for the ECM process with direct current are also applicable for the PECM process. Kozak et al. demonstrated this in a one dimensional model of the flow channel [10]. It allows the selection of machining parameters that prevent boiling of the electrolyte while maximizing the removal rate. However, the model neglects convective heat transfer during pulse interval time and does therefore overestimate the electrolyte heating. Furthermore, the extension to two or even three dimensions is practically hindered by immense computational costs. The reason lies in the additional time scales involved in the PECM process. In ECM with direct current, all state variables vary in dependence of geometry changes due to cathode feed and anodic dissolution. Consequently, they change with the time scale of the machining task that typically lasts in the range of 1 000 s. For the simulation this means that a step size of about 50 ms, or a frequency of 20 Hz respectively, is sufficient [11] to reproduce all physical phenomena. The PECM process, in contrast, is characterized by three different time scales that are shown in Figure 1. During the process, the cathode position is altered with a frequency of up to 100 Hz. The simulation step size would have to be significantly smaller to reproduce changes of the velocity field and the gap width. The electric current even varies in the range of 1 000 Hz. Choosing a suitable step size to reproduce this effect would result in a simulation step size in the range of 0.1 ms or lower. Thus, the computational costs increase by a factor of 500 compared to the ECM process with direct current. In conclusion, it is practically not possible to simulate each electric pulse or even mechanical oscillation. Instead, short-cut methods have to be applied to reduce the simulation costs.

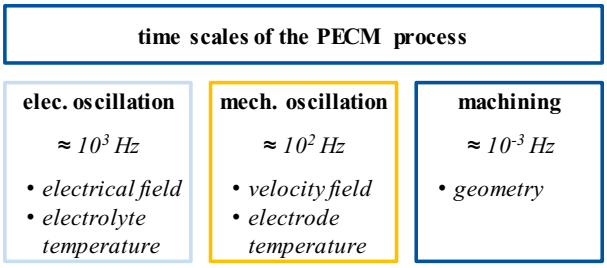

Fig. 1. Time scales of typical PECM processes

Smets et al. introduced such a method for the simulation of the temperature field during pulsed ECM [12]. Their quasi steady state short-cut method decomposes the temperature evolution in an average temperature, a ripple and a decaying component. They showed that delaying the electric pulses with a time interval allows neglecting the decaying component. Thereby, the quasi steady state temperature field can be calculated with fewer time steps. However, the approach does not include a model of the material removal and can thus not predict the machined geometry.

In order to include the material removal, Hackert-Oschätzchen et al. further simplified the model [13]. By multiplying the simulated current density by the duty cycle they obtained the average current. In that way, they could model the pulsed ECM process like an ECM process with direct current. However, when the average current is applied the average heat will not be produced due to non-linear relationships [12].

This disadvantage is overcome by the averaging algorithm of Hotoiu and Deconinck [14]. The algorithm is structured in two nested loops. The inner loop, called “pulse loop”, simulates the temperature distribution and the electric current for a few pulses. Subsequent, the average electric charge and heat source are computed and passed to the outer loop called “temperature and deformation loop”. The outer loop uses these boundary conditions to simulate the dissolution as well as the temperature field of several pulses. These results are again passed to the inner loop. This procedure significantly reduces number of time steps that have to be calculated.

None of the three short-cut methods presented above consider a varying flow channel height induced by the cathode oscillation. Thus, they cannot be directly applied to the PECM process. Nevertheless, the algorithm by Hotoiu and Deconinck can be adapted in order to include the cathode oscillation. In the model of Schaarschmidt et al. the inner loop simulates the velocity field, the temperature field, the gas evolution and the electric field during one oscillation [4]. Subsequent, the

average removal velocity is passed to the outer loop that computes the geometry after 30 s of machining. The new geometry is passed to the inner loop again. This model enables the simulation of two-dimensional geometries in a sufficient amount of time. However, the model still has two shortcomings. First, the velocity field is modeled as a potential flow to reduce the computational costs. Because this approach does not consider friction in the electrolyte, it cannot model boundary layers which have a significant influence of the temperature field of the electrolyte [11]. Second, the step size of 30 s is chosen arbitrarily and constant. The model does not include a criterion to evaluate the quality of the step size.

Finally, it should be mentioned that no model for neither PECM nor pulsed ECM processes has been validated by comparing geometries obtained in simulation and experiment.

3. New Modeling Approach

Based on the models discussed in the previous section a new modeling approach is presented. First, the model equations describing the individual physical phenomena are outlined. Second, the division into three simulation steps to handle different time scales is introduced. Third, the geometry and machining parameters that were used for the simulation are presented.

3.1. Model equations

Equations used to model the physical phenomena of the ECM process have repeatedly been described by various authors. The model presented in this paper is based on [15] where a detailed description of the equations is given. The electric field is modeled by the Maxwell equations while considering the linear temperature dependency of the electrical conductivity of the electrolyte. Polarization voltages were determined experimentally. The electrolyte flow is described by the Navier-Stokes equations. Turbulent flow is taken into account by the k-ε-model. Fourie's law and energy conservation are applied to model the temperature field. Material removal is computed based on Faraday's law while the effective material removal was experimentally determined.

3.2. Simulation steps and time stepping

The simulation is divided into three consecutive simulations steps, which are represented in Figure 2. As a first step, the stationary velocity field of the electrolyte is simulated at the BoP (u_{BoP}) and the BDC (u_{BDC}). Subsequently, the velocity field at any other point in time during the pulse packet is linearly interpolated based on the cathode position:

$$u(z) = u_{BDC} \cdot \frac{z(t)-z_{BoP}}{z_{BDC}-z_{BoP}} + u_{BoP} \cdot \left(1 - \frac{z(t)-z_{BoP}}{z_{BDC}-z_{BoP}}\right). \quad (1)$$

Hereby, the costly transient simulation of the fluid field is omitted. The interpolation is based on the assumptions that changes of the velocity field due to the changing flow channel height appear instantly and that the flow condition during one pulse packet does not change its character. The second simulation step computes the transient solution of the electric field and the temperature evolution during one pulse packet while considering the changing flow channel height due to mechanical oscillation. Subsequently, the current density at each mesh element of the electrolyte-anode interface is integrated over time from BoP to EoP. The resulting electrical charge Q_j is passed to the third simulation step that determines the material dissolution and the new anode geometry. The geometry in turn is passed to the first simulation step to start a new simulation cycle.

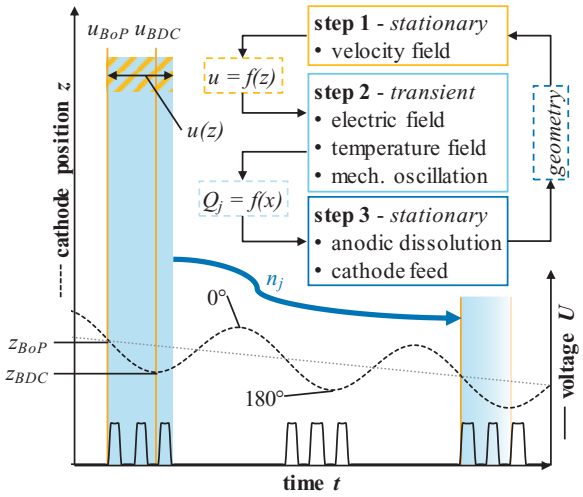

Fig. 2. Simulation procedure of the new modeling approach

Since the electrical charge flowing during one pulse packet hardly differs within a row of consecutive oscillations the geometry change can be calculated for several mechanical oscillations at once. Therefore, the electrical charge calculated in simulation step two is multiplied by the number of oscillations. In former publications (cp. [4]) this step size n_j was set to an arbitrary and constant value. However, a reasonable step size may differ during the simulation progress. For example, in the beginning of the simulation when the quasi-static flow channel height is not yet reached, faster changes in the electrical charge can be expected and the step size should be kept small. Later in the machining progress, higher step sizes should be applied to reduce the duration of simulation. Therefore, a criterion ΔQ_j was defined that a posteriori evaluates the quality of the chosen step size. It describes to what extent the electric field changes within on simulation cycle:

$$\Delta Q_j = \sqrt{\int_0^{x_{max}} \left(Q_j - Q_{j-1}\right)^2 dx}. \quad (2)$$

Q_j and Q_{j-1} are the electrical charges calculated in step two of the current and the previous simulation cycle respectively. The integration is executed on the electrolyte anode interface. Based on this criterion a formula is introduced that gives the step size for the current simulation cycle:

$$n_j = n_{j-1}\left(2 - \frac{\Delta Q_j}{0.01}\right). \quad (3)$$

If ΔQ_j is smaller than 0.01 the step size is increased. If ΔQ_j is larger than 0.01 the step size is decreased. Thereby the change in the electrical charge between two simulation cycles is kept at around 1 %.

3.3. Geometry and Materials

For the simulation of the PECM machining with the presented model a two-dimensional reference geometry was defined. As shown in Figure 3, the electrolyte channel (I) has an inlet with a height of 3 mm. The workpiece (II) measures 6 mm in height and 16 mm in length and the cathode (III) consists of two ellipse quarters with semi axes of 6 mm and 0.5 mm.

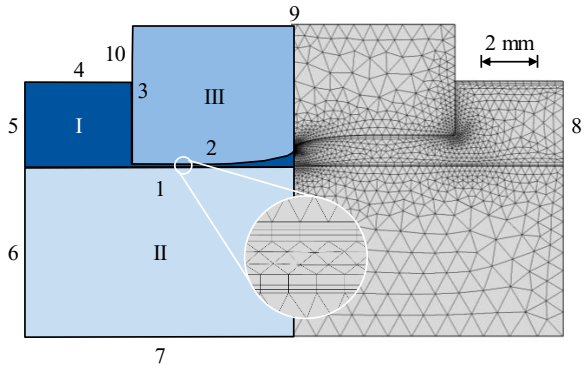

Fig. 3. Reference geometry and mesh

This geometry was chosen to investigate curvatures and dimension which are typical for blades in the high-pressure compressor of aircraft engines. Accordingly, direct aged Inconel 718 was defined as workpiece material and a sodium nitrate based electrolyte was chosen. The respective material parameters are listed in Table 1.

Table 1. Material parameters

	Material	Density ρ / (kg/m^3)	Elec. cond. κ / (S/m)	Therm. cond. λ / (W/(m·K))	Heat capacity c_p / (J/(kg·K))
I	$NaNO_3$ elect.	1000	*f(T)*	0.594	4187
II	Inconel 718	8228	$8 \cdot 10^5$	10.42	432
III	Copper	8960	$6 \cdot 10^7$	400	385

3.4. Simulation mesh and parameters

The applied mesh is shown in Figure 3 on the right hand side. It consists of roughly 10 000 elements. However, the exact number of elements differs between simulation cycles because a new mesh is built for each geometry computed in simulation step 3. In accordance with [4, 11] the height of the flow channel is discretized by eleven elements.

The machining parameters, which are listed in Table 2, are typical for PECM processes. Electric frequency and duty cycle are equivalent to a pulse duration of 0.625 ms and a pulse interval time of 1 ms. Thus, four electric pulses are triggered during one oscillation.

Table 2. Machining and simulation parameters

Parameter	Value
electric parameters	
working voltage U	15 V
electric frequency f_e	600 Hz
duty cycle τ	37.5 %
begin of pulse packet *BoP*	100°
end of pulse packet *EoP*	210°
mechanical parameters	
feed rate v	0.2 mm/min
maximum sinking depth z_{max}	1.5 mm
frequency of oscillation f_m	50 Hz
amplitude of oscillation $\hat{s}$	100 µm
initial gap size s_0	100 µm
electrolyte parameters	
inlet pressure p_{in}	7.5 bar
outlet pressure p_{out}	5 bar
inlet temperature T_{in}	293.15 K
simulation parameters	
sum of polarization voltage ΔU	3.6 V
specific material removal v_{eff}	1.51 mm^3/(A·min)
electric conductivity at 20°C κ_0	10 S/m
temperature slope of conductivity $\Delta\kappa$	0.231 S/(m·K)
ambient temperature $T_{ambient}$	293.15 K
initial step size n_0	25

4. Simulation Results

The following section presents the simulation results subdivided into the three simulation steps. It focuses on the evaluation of the two introduced short cut methods.

4.1. Step 1 - Velocity field

The velocity field determines the convective heat transfer during the PECM process and is therefore essential for the second simulation step. Figure 4 shows the flow rate during one pulse packet at three different points of the machining process. The electrolyte flow through the gap significantly changes and follows the mechanical oscillation. At a machining progress of 1 mm the difference between the minimal and maximal flow rate is 38 %. This illustrates the necessity to consider the varying velocity field during oscillation. Furthermore, the flow rate also changes following the machining progress. Due to the chosen geometry, the flow channel length continuously increases which results in a growing flow resistance. Consequently, the minimal flow rate decreases from 314 mm^2/min at machining progress of 0.5 mm to 197 mm^2/min at the end of machining.

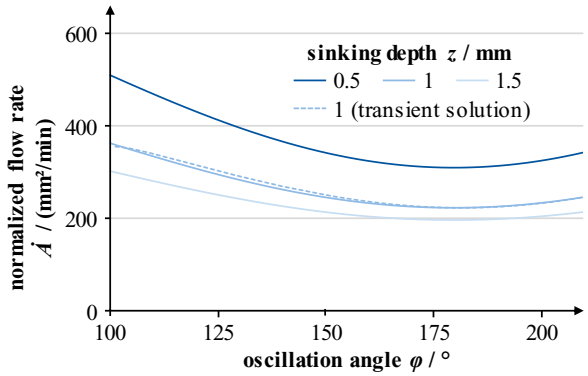

Fig. 4. Flow rate during one oscillations at three different points of machining

In order to validate the interpolation method for the velocity field (cp. equation (1)) a transient simulation of the velocity field during one oscillation at a machining progress of 1 mm was performed. The computed flow rate is also shown in Figure 4. It becomes apparent that variation between the interpolated and the transient solution is negligibly small. For further validation, Figure 5 depicts both solutions at an oscillation angle of 140° that represents the point furthest from the stationary solutions of the velocity field (cp. Figure 2). Both solutions qualitatively differ little from each other. The standardized square deviation, in contrast, shows high deviations in the regions of low electrolyte velocity that even exceed 100 %. Nevertheless, the regions do not occur in the flow channel and do therefore not have a significant influence on the machining result. In the flow channel, the quantitative deviations do not exceed 15 %. Thus, it can be concluded that the interpolation method for the velocity field presented in this paper is a valid short-cut method for the simulation of the PECM process.

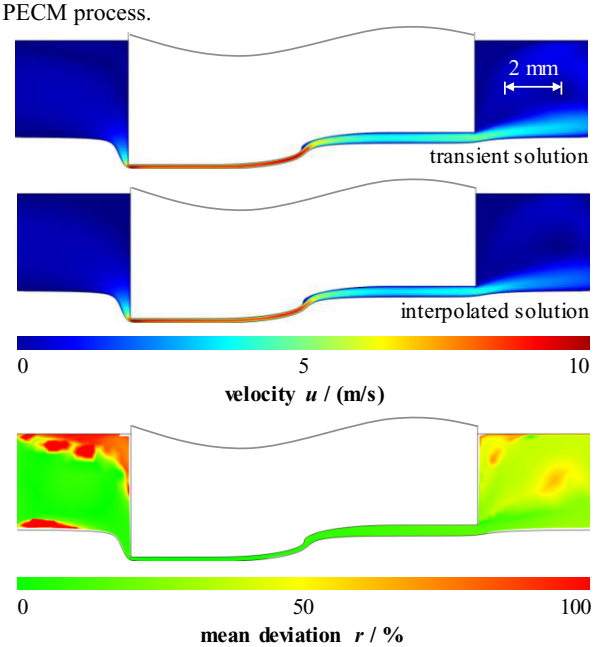

Fig. 5. Transient and interpolated solution of the velocity field and their standardized square deviation at a sinking depth of z = 1 mm

4.2. Step 2 - Temperature field and electrical field

The electrolyte temperature determines the electrical conductivity and thus influences the resulting workpiece shape. Figure 6 shows the temperature field at a cathode feed of 1.5 mm. The oscillation angle is φ = 182.5° which corresponds to the beginning of the last electrical pulse within one pulse packet. It becomes apparent that the interval time between two electrical pulses is not sufficient to exchange the electrolyte in the whole flow channel. In the left half of the flow channel, fresh electrolyte has decreased the temperature to inlet temperature while the temperature of the right half of the flow channel is about 12 K higher.

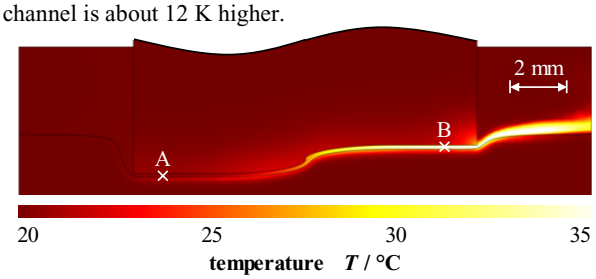

Fig. 6. Development of temperature and current density during one pulse packet at the end of machining (z = 1.5 mm)

In order to further evaluate this phenomenon Figure 7 shows the development of temperature and current density during one pulse packet at points A and B (see Figure 6). At both points, the current density rises during the first three pulses due to the narrowing flow channel. Since the last pulse lies past the BDC the current density is slightly lower than during the third pulse. In addition, current density rises during each single pulse because of the rising temperature. However, there is a distinct difference between point A and B. At point A temperature nearly returns to inlet temperature at the beginning of each pulse. At point B in contrast the heat accumulates. Consequently, the current density increases stronger at point B than at point A.

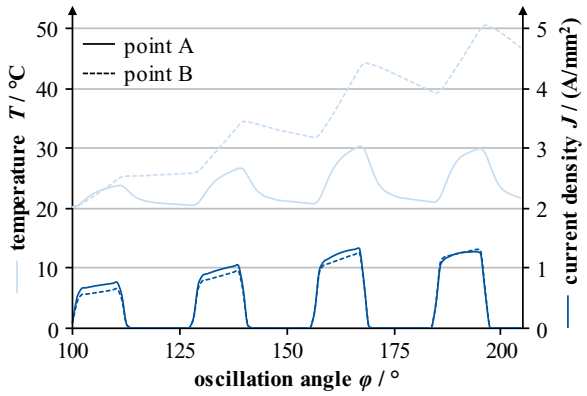

Fig. 7. Development of temperature and current density during one pulse packet at the end of machining (z = 1.5 mm)

4.3. Step 3 - Time stepping and resulting geometry

The final simulation step uses the computed electrical charge to determine the resulting workpiece geometry. Figure 8

shows the flow channel height at the end of machining. Naturally, the shoulder in the middle of the cathode leads to a widening of the gap. Moreover, the gap at the second half of the cathode is 20 µm wider than at the first half. This agrees with the finding that heat accumulates at the second half. In future work the computed flow channel height could be used to adapt the cathode in order to achieve a desired workpiece shape.

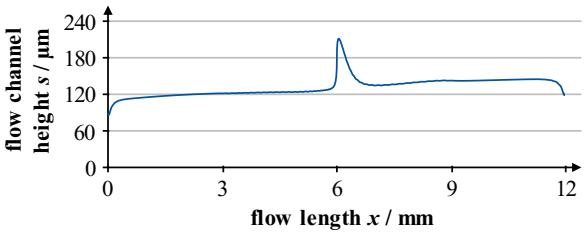

Fig. 8. Flow channel height s at the end of machining (z = 1.5 mm)

In section 3.2 a new time stepping algorithm was introduced that varies the step size between simulation cycles. Figure 9 shows the development of the step size as well as the criterion ΔQ_j during the simulation progress. Evidently, the algorithm succeeds to keep the change of the current density between two simulation steps at about 1 %. At first, the steps size increases while the left half of the cathode approaches the quasi steady state. However, when the right half of the cathode approaches the workpiece surfaces the current density distribution changes and the step size has to be decreased in order to limit the change in current density between two simulation cycles. Shortly before the end of the simulation, the step size can be increased again because the right half of the cathode also reaches quasi steady state.

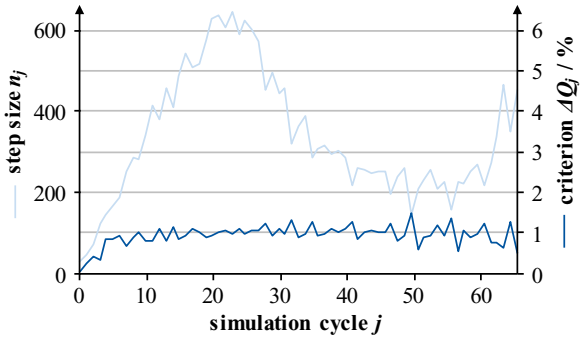

Fig. 9. Step size and criterion ΔQ_j during the simulation progress

5. Summary and Outlook

The different time scales involved in the PECM make it challenging to simulate the process temporally fully resolved. Nevertheless, a fast simulation tool could decrease costs and duration of the cathode design process in PECM. This paper evaluated existing approaches and deducted a novel modeling approach that is characterized by two short cut methods. First, the velocity field was interpolated from two stationary solutions. Second, a time stepping algorithm has been introduced to allow a adaptive step size during the simulation of the material dissolution.

In further work the model will be validated by machining a cavity with the defined reference cathode and compare the simulated and machined workpiece shape. In case no sufficient agreement is found, the model should be extended by including the influence of gas evolution during the PECM process.

Finally, it has to be concluded that the development of further short cut methods is necessary. With the presented model, the simulation of the relatively simple reference geometry took about 48 hours. For geometries that are more complex or even three-dimensional simulations the duration would unacceptably increase. A possible approach could be to directly deduct the electrical field from the velocity field to omit simulation step 2.

References

[1] Klocke, F., Klink, A., Veselovac, D., Aspinwall, D.K. *et al.*, 2014. Turbomachinery component manufacture by application of electrochemical, electro-physical and photonic processes. CIRP Annals - Manufacturing Technology *63*, p. 703.

[2] Hinduja, S., Kunieda, M., 2013. Modelling of ECM and EDM processes. CIRP Annals - Manufacturing Technology *62*, p. 775.

[3] Klocke, F., Zeis, M., Klink, A., 2015. Interdisciplinary modelling of the electrochemical machining process for engine blades. CIRP Annals - Manufacturing Technology *64*, p. 217.

[4] Schaarschmidt, I., Zinecker, M., Hackert-Oschätzchen, M., Meichsner, G. *et al.*, 2017. Multiscale Multiphysics Simulation of a Pulsed Electrochemical Machining Process with Oscillating Cathode for Microstructuring of Impact Extrusion Punches. Procedia CIRP *58*, p. 257.

[5] Tipton, H., 1971. *The determination of the shape of tools for the use in electrochemical machining*. M.I.R.A, Macclesfield.

[6] Riggs, J., Muller, R., Tobias, C., 1981. Prediction of work piece geometry in electrochemical cavity sinking. Electrochimica Acta *26*, p. 961.

[7] Kozak, J., Dabrowski, L., Lubkowski, K., Rozenek, M. *et al.*, 2000. CAE-ECM system for electrochemical technology of parts and tools. Journal of Materials Processing Technology *107*, p. 293.

[8] Fujisawa, T., Inaba, K., Yamamoto, M., Kato, D., 2008. Multiphysics Simulation of Electrochemical Machining Process for Three-Dimensional Compressor Blade. Journal of Fluids Engineering *130*, p. 81602.

[9] Deconinck, D., van Damme, S., Deconinck, J., 2012. A temperature dependent multi-ion model for time accurate numerical simulation of the electrochemical machining process. Part I: Theoretical basis. Electrochimica Acta *60*, p. 321.

[10] Kozak, J., Rajurkar, K.P., Ross, R.F., 1991. Computer simulation of Pulse Electrochemical Machining (PECM). Journal of Materials Processing Technology *28*, p. 149.

[11] Zeis, M., Klocke, F., 2015. *Modellierung des Abtragprozesses der elektrochemischen Senkbearbeitung von Triebwerksschaufeln,* 1st edn. Apprimus-Verl., Aachen.

[12] Smets, N., van Damme, S., Wilde, D. de, Weyns, G. *et al.*, 2008. Time averaged temperature calculations in pulse electrochemical machining, part II: Numerical simulation. Journal of Applied Electrochemistry *38*, p. 551.

[13] Hackert-Oschätzchen, M., Kowalick, M., Zinecker, M., Kuhn, D. *et al.*, 2016. 2-D Axisymmetric Simulation of the Electrochemical Machining of Internal Precision Geometries, in *Introduction to statistical machine learning*, Morgan Kaufmann Publishers, Waltham, MA, p. 1.

[14] Hotoiu, L., Deconinck, J., 2013. Time-Efficient Simulations of Nano-Pulsed Electrochemical Micro- Machining. Procedia CIRP *6*, p. 469.

[15] Klocke, F., Zeis, M., Harst, S., Klink, A. *et al.*, 2013. Modeling and Simulation of the Electrochemical Machining (ECM) Material Removal Process for the Manufacture of Aero Engine Components. Procedia CIRP *8*, p. 265.